

## SOME NEW DEVELOPMENTS OF POLYNOMIAL PRESERVING RECOVERY ON HEXAGON AND CHEVRON PATCHES

HAO PAN, ZHIMIN ZHANG, AND LEWEI ZHAO

**Abstract.** Polynomial Preserving Recovery (PPR) is a popular post-processing technique for finite element methods. In this article, we propose and analyze an effective linear element PPR on the equilateral triangular mesh. With the help of the discrete Green's function, we prove that, when using PPR to the linear element on a specially designed hexagon patch, the recovered gradient can reach  $O(h^4 |\ln h|^{\frac{1}{2}})$  superconvergence rate for the two dimensional Poisson equation. In addition, we apply PPR to the quadratic element on uniform triangulation of the Chevron pattern with an application to the wave equation, which further verifies the superconvergence theory.

**Key words.** Finite element method, post-processing, gradient recovery, superconvergence.

### 1. Introduction

In recent years, since the development of the high accuracy post-processing and a posteriori error estimate ([1] and [2]), there has been growing interest in the superconvergence and other kinds of high accuracy methods such as defect correction and extrapolation. Finite element recovery techniques are post-processing methods that reconstruct numerical approximations from finite element solutions to achieve better results. We consider only  $C^0$  finite element methods, although generalization to other finite element methods, such as non-conforming and discontinuous Galerkin methods, are feasible. Let  $u$  be a solution of certain differential equation, and  $u_h$  be the finite element approximation of  $u$ . The goal of a recovery technique is to construct  $G_h u_h$  based on  $u_h$  such that  $G_h u_h$  is a better approximation of  $\nabla u$  than  $\nabla u_h$ . Naturally, the mathematical background of recovery techniques is closely related to the finite element superconvergence theory, see, e.g., the monographs [3] and [4].

Zienkiewicz and Zhu first introduced the gradient recovery method Superconvergence Patch Recovery (SPR, ([5]) in 1992 based on a local discrete least-squares fitting. Later, Zhang and Naga proposed an alternative strategy ([6]) called Polynomial Preserving Recovery (PPR) to recover the gradient. Theoretical analysis reveals that PPR has better superconvergence properties than SPR ([7]). It has been implemented by commercial finite element software COMSOL Multiphysics as a superconvergence tool. There have been further developments on applications of PPR in numerical methods. For example, Guo and Yang ([8]) generalized the study of PPR to high-frequency wave propagation in 2016. Wang et al. establish the superconvergence for Maxwell equations and combine with PPR that leads to global superconvergence for recovered quantities in energy norms ([9]). Du and Zhang study the supercloseness property of the linear Discontinuous Galerkin finite element method and its superconvergence behavior after post-processing by the PPR ([10]). Guo et al. generalized the idea of PPR to the general polygons, which only uses the degrees of freedom and has the consistency on arbitrary polygonal meshes

by the polynomial preserving property([11]). They prove the polynomial preserving and boundedness properties of the generalized gradient recovery operator.

In practice, PPR is performed on an element patch  $\omega_z$  (around  $z$ ) which is a union of elements that covers all nodes needed for the construction of  $G_h u_h(z)$ . Different mesh patterns and selection of patches result in different recovery. Some popular mesh patterns include the regular pattern, the Chevron pattern, the Union-Jack pattern, etc. ([6] and [7]). In general, PPR can attain  $h^2$  superconvergence rate for the recovered gradient at an element vertex  $z$  for the linear element (Theorem 8.17 of [7]). In this article, we design a hexagon patch on equilateral triangulation (Section 3.1) to reach a surprising superconvergence rate  $h^4 |\ln h|^{\frac{1}{2}}$  for the recovered gradient from the linear element (Theorem 7). Standard approximation theory fails to prove such a higher order superconvergence. In order to prove our theory, we use the asymptotic error expansion in [12] and interior maximum norm estimates for the discrete Green's function in Section 3.2. Furthermore, an equal superconvergence phenomenon is found on equilateral triangulation (Theorem 8). In addition, we apply PPR to the quadratic element on the uniform triangulation of the Chevron pattern, which further verifies the superconvergence stated in Theorem 3.1 in [6]. We also perform the quadratic PPR numerical experiments for a wave equation on the Chevron pattern mesh.

An outline of this paper is as follows. We devote Section 2 to existed theory for PPR. The general set up for the linear element PPR on the Hexagon patch is then constructed in Section 3. Finally the applications of the PPR to the quadratic element on the uniform triangulation of the Chevron pattern are presented in Section 4.

**2. Some preliminaries of PPR**

In this section, we introduce some basic knowledge of PPR in 2D. We consider the following variational problem on a polygonal domain  $\Omega$  : Find  $u \in H_0^1(\Omega)$  such that

$$(1) \quad a(u, v) = f(v), \quad \forall v \in H_0^1(\Omega),$$

where

$$a(u, v) = \int_{\Omega} [(A \nabla u + bu) \cdot \nabla v + cuv].$$

We assume that all the coefficient functions are smooth,  $A$  is a  $2 \times 2$  symmetric positive definite matrix,  $f(\cdot)$  is a linear functional, and the bilinear form is continuous and satisfies the inf-sup condition (8.3.14)-(8.3.15) of [7] on  $H^1(\Omega)$ .

Let  $T_h = \{K\}$  be a finite regular triangulation of  $\Omega$  of width  $h$  with all its boundary vertices on  $\partial\Omega$ . Corresponding to  $T_h$ , we define the following finite element spaces:

$$S_h(\Omega) = \{v_h \in C(\Omega_h) : v_h \text{ is piecewise polynomial of degree} \leq k \text{ on each } K \in T_h\}$$

$$S_h^0(\Omega) = \{v \in S_h : \text{supp}(v) \in \Omega_h\}.$$

where  $\Omega_h = \cup\{K \in T_h\}$ . Then the finite element approximation  $u_h \in S_h^0(\Omega)$  satisfies

$$(2) \quad a(u_h, v) = f(v), \quad \forall v \in S_h^0(\Omega_h).$$

To ensure the uniqueness of the finite element solution, we assume the discrete inf-sup condition (8.3.17) of [7].

Given a node  $z$ , we select  $n \geq (k + 2)(k + 3)/2$  sampling points adjacent to  $z$ , and fit a polynomial of degree  $k + 1$ , in the least square sense, with values of  $u_h$  at

those sampling points. In other words, we are looking for  $p_{k+1} \in P_{k+1}$  such that

$$\sum_{j=1}^n (p_{k+1} - u_h)^2(z_j) = \min_{q \in P_{k+1}} \sum_{j=1}^n (q - u_h)^2(z_j).$$

The PPR recovers the gradient at  $z$ , and is defined as

$$G_h u_h(z) = \nabla p_{k+1}(z).$$

It was proved in [13] that certain rank condition and geometric condition guarantee the uniqueness of  $p_{k+1}$ , and  $G_h$  is a linear operator from  $S_h$  to  $S_h \times S_h$ . We list three important properties of  $G_h$  below. Their proof and other properties can be found in [6] and [7].

**Proposition 1.** *(Polynomial preserving)  $G_h$  is polynomial preserving in the sense that  $G_h u_I = \nabla u$  for any  $u \in P_{k+1}$ , where  $u_I \in S_h$  is the Lagrange interpolation of  $u$ . If  $z_i$  is a mesh symmetry center of involved nodes and  $k = 2r$ , then  $G_h$  preserves polynomials of degrees up to  $k + 2$  at  $z_i$ .*

**Proposition 2.** *Let the coefficients in the differential operator given in (1) be constants, and let the finite element space, which includes piecewise polynomials of degree  $k$ , be translation invariant in directions on  $\Omega$ , and let  $u \in W^{k+2,\infty}(\Omega)$ . Assume  $u_h \in S_h$  is the finite element solution of (2). Assume further that Theorem 5.5.2 in [4] is applicable. Then on any interior region  $\Omega_0 \subset \subset \Omega$ ,*

$$\|\nabla u - G_h u_h\|_{L^\infty(\Omega_0)} \lesssim (\ln \frac{1}{h})^{\bar{r}} h^{k+1} \|u\|_{W^{k+2,\infty}(\Omega)} + \|u - u_h\|_{W^{-s,q}(\Omega)},$$

for some  $s \geq 0$  and  $q \geq 1$ .

**Proposition 3.** *Consider an interior patch  $\omega_z \in \Omega_d \subset \Omega_{1,h}$  with  $d = \text{dist}(\omega_z, \partial\Omega_d) \geq Kh$  for some constant  $K > 0$ . Let  $u \in H^3(\Omega) \cap W^{2,\infty}(\Omega)$  and  $u_h \in S_h$  be the exact and the linear element solution of (1) and (2), respectively. Assume Condition  $(\alpha, \sigma)$  is satisfied. Then*

$$|(\nabla u - G_h u_h)(z)| \lesssim h^{1+\min(1,\alpha)} \|u\|_{3,\infty,\omega_z} + d^{-1} h^2 \ln \frac{1}{h} \|u\|_{2,\infty,\Omega} + h^{1+\alpha} \ln \frac{d}{h} \|u\|_{2,\infty,\Omega_d}.$$

In view of Proposition 3, linear element PPR can reach the order of 2 for a general patch. In the next section, we will construct a new special patch in the equilateral triangle mesh to get ultraconvergence as  $h^4 |\ln h|^{\frac{1}{2}}$ .

### 3. Linear element PPR on the Hexagon patch in equilateral triangle mesh

**3.1. A new PPR patch.** For the linear element in equilateral triangle mesh, performing the discrete least squares fitting, we obtain the coefficients of the cubic polynomial at 13 vertices ( $P_j, j=0\dots 12$ ) of the scaled patch  $\omega_z$  in Figure 1: vertex 0 is the patch center  $z$ , vertex 1 to 6 are adjacent to the center, and vertex 7 to 12 are other vertices. Thereby recovering the gradient of  $u$  with  $G_h u_h(x, y) = \nabla p_3(x, y)$  on the patch  $\omega_z$ .

$$(3) \quad G_h u_h(z) = \sum_{j=0}^{12} \frac{c_j u_h(P_j)}{h},$$

where  $\sum_{j=0}^{12} c_j = 0$  by Proposition 8.6 of [7].

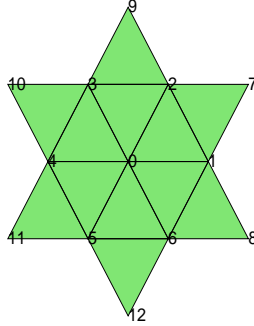


FIGURE 1. The linear element PPR for  $G_h u_h = \nabla p_3$ .

Let  $p_3(z) = u_o + a_1x + a_2y + a_3x^2 + a_4xy + a_5y^2 + a_6x^3 + a_7x^2y + a_8xy^2 + a_9y^3$ , then in the local reference coordinate  $G_h u_h(0, 0) = \nabla p_3(0, 0) = (a_1, a_2)$ ,

$$(4) \quad \begin{aligned} G_{hx}u_h(0, 0) &= \frac{1}{2h} [(u_1 - u_4) + (\frac{u_2 + u_6}{2} - \frac{u_3 + u_5}{2})] + \frac{1}{6h} (\frac{u_{10} + u_{11}}{2} - \frac{u_7 + u_8}{2}), \\ G_{hy}u_h(0, 0) &= \frac{\sqrt{3}}{2h} [(\frac{u_2 + u_3}{2} - \frac{u_5 + u_6}{2}) + \frac{1}{9}(u_{12} - \frac{u_7 + u_{10}}{2}) + \frac{1}{9}(\frac{u_8 + u_{11}}{2} - u_9)], \\ u_j &= u_h(P_j). \end{aligned}$$

By Taylor expansion analysis,

$$(5) \quad \begin{aligned} |(G_{hx}u_I - \frac{\partial u}{\partial x})(0, 0)| &= \frac{1}{80}h^4 \frac{\partial^5 u}{\partial x^5}(0, 0) + O(h^6), \\ |(G_{hy}u_I - \frac{\partial u}{\partial y})(0, 0)| &= \frac{3}{160}h^4 \frac{\partial^5 u}{\partial y^5}(0, 0) + O(h^6). \end{aligned}$$

To analyze the error, we decompose

$$(6) \quad \nabla u - G_h u_h = (\nabla u - G_h u_I) + G_h(u_I - u_h).$$

Then the first term  $|(\nabla u - G_h u_I)(z)| \leq Ch^4$  by Taylor approximation (5). So we only need to consider the second term  $|G_h(u_h - u_I)|$ .

**3.2. Interior estimates for the discrete Green’s function.** From the view of (3), the recovery operator  $G_h$  is a linear combination of the solution values  $u_h(P_j)$ , which is divided by  $h$ . By Proposition 8.7 in [7],  $G_h$  is a bounded operator in the sense

$$(7) \quad |G_h v(z)| \lesssim |v|_{W^{1,\infty}(\omega_z)}, \quad \forall v \in S_h.$$

So by directed analysis,

$$|G_h(u_h - u_I)(z)| \leq |G_h||u_h - u_I|_{W^{1,\infty}(\omega_z)}.$$

The derivative will cause the error estimation to lose one order less than the superconvergence rate we expect. To overcome such a difficulty, we adopt the interior estimate technique in the superconvergence analysis of [6] and the proof of Theorem 8.17 in [7]. We introduce a separation parameter  $d = \text{dist}(\omega_z, \partial\Omega_d) \geq Kh$  for some constant  $K$  to separate  $\omega_z \subset \subset \Omega_d \subset \Omega$  such that this loss in one order  $h^{-1}$  is replaced by fixed  $d^{-1}$  to obtain the expected superconvergence. Motivated by this

technique, we now set up the interior estimates for the discrete Green's function that will be used in the proof of superconvergence.

**Definition 4.** Let  $g_h^z \in S_h^0$  be the discrete Green's function defined by (1.10) of [3] :

$$(8) \quad a(g_h^z, v) = v(z) \quad \forall v \in S_h^0(\Omega).$$

The analysis in this section closely follows the argument of Lemma 3.2 in [14]

**Lemma 5.** For bounded domains  $\Omega_0$  and  $\Omega_d$  with  $\Omega_0 \subset\subset \Omega_d$ , where  $d = \text{dist}(\partial\Omega_0, \partial\Omega_d)$ . We shall assume that the meshes are locally quasi-uniform of size  $h$ ; we shall then require  $d \geq Kh$  for  $K > 0$  large enough, then

$$(9) \quad \|g_h^z\|_{W^{1,\infty}(\Omega_0)} \lesssim d^{-1} |\ln h|^{\frac{1}{2}}.$$

*Proof.* It suffices to prove our result with  $\Omega_0$  replaced by a ball  $B_d$  and  $\Omega_d$  by a concentric ball  $B_{3d}$ . We scale this situation by introducing a new variable  $y = x/d$ , we have with  $\tilde{g}_h^z(y) = g_h^z(yd)$ .

It is elementary to check that

$$(10) \quad |g_h^z|_{W^{1,\infty}(B_d)} + d^{-1} \|g_h^z\|_{L^\infty(B_d)} = d^{-1} \|\tilde{g}_h^z\|_{W^{1,\infty}(B_1)}.$$

We shall also let  $\tilde{\delta} = \tilde{\delta}_{j,x_0}$  ( $j = x, y$ ) be such that, for  $x_0 \in B_1$ ,

$$D_j v(x_0) = (D_j v, \tilde{\delta}) \quad \forall v \in S_h.$$

We let  $V \in H^1(B_3)$  be defined by (3.10) in [14] and the projection  $\Pi V \in S_h(B_3)$  given by

$$a(V - \Pi V, v) = 0 \quad \forall v \in S_h.$$

We then obtain, for  $x_0 \in B_1$ ,

$$(11) \quad D_j \tilde{g}_h^z(x_0) = (D_j \tilde{g}_h^z, \tilde{\delta}) = -(\tilde{g}_h^z, D_j \tilde{\delta}) = a(\tilde{g}_h^z, V) = a(\tilde{g}_h^z, \Pi V).$$

Now let  $\chi_h \in \tilde{S}^h(B_{1.4})$  with  $\chi_h = \Pi V$  in  $B_{1.3}$  such that

$$(12) \quad \|\Pi V - \chi_h\|_{H^1(B_{1.5} \setminus B_{1.3})} \lesssim \|\Pi V\|_{H^1(B_{1.5} \setminus B_{1.2})}.$$

Such a  $\chi_h$  exists by Lemma 2.3 of [14]. From (11) we then have

$$(13) \quad D_j \tilde{g}_h^z(x_0) = a(\tilde{g}_h^z, \Pi V - \chi_h) + \chi_h(z).$$

Here, by (12)

$$(14) \quad |a(\tilde{g}_h^z, \Pi V - \chi_h)| \lesssim \|\tilde{g}_h^z\|_{H^1(B_{1.5})} \|\Pi V\|_{H^1(B_{1.5} \setminus B_{1.2})}.$$

By Theorem 3.5 of [3]

$$(15) \quad \|\tilde{g}_h^z\|_{H^1(B_{1.5})}^2 \lesssim |\ln h|.$$

Further, since  $a(v, \Pi V) = 0$  for  $v \in \tilde{S}^h(B_2 \setminus B_{1.1})$ , from Lemma 2.6 of [14], we obtain

$$(16) \quad \|\Pi V\|_{H^1(B_{1.5} \setminus B_{1.2})} \lesssim \|\Pi V\|_{W^{1,1}(B_3 \setminus B_{1.1})}.$$

Using Lemma 2.1 and Lemma 3.1 in [3], we conclude that

$$(17) \quad \|\Pi V\|_{W^{1,1}(B_3 \setminus B_{1.1})} \lesssim \|V\|_{W^{1,1}(B_3 \setminus B_{1.1})} + \|V - \Pi V\|_{W^{1,1}(B_3)} \leq C.$$

Hence, from (14)-(17)

$$(18) \quad |a(\tilde{g}_h^z, \Pi V - \chi_h)| \lesssim |\ln h|^{\frac{1}{2}}.$$

From (13) and (18), we now have

$$|D_j \tilde{g}_h^z(x_0)| \lesssim |\ln h|^{\frac{1}{2}}.$$

Then we obtain (9) from (10). □

**3.3. Asymptotic error expansion for linear finite elements on equilateral triangulation.** This part is based on Blum, Lin and Rannacher’s result in 1986 ([12]). They showed the elliptic Ritz projection with linear finite elements to admit asymptotic error expansions on certain uniform meshes. Its success depends on the presence of an asymptotic error expansion of the type

$$u_h(z) = u(z) + \sum_{k=1}^n h^{2k} e^{(k)}(z) + o(h^{2n})$$

in mesh points  $z$ , where the coefficients  $e^{(k)}(z)$  are independent of the mesh size parameter  $h$ . They consider the model Dirichlet problem

$$(19) \quad \begin{aligned} -\Delta u &= f \quad \text{in } \Omega, \\ u &= b \quad \text{on } \partial\Omega, \end{aligned}$$

where  $\Omega$  is a polygonal domain, and  $f$  and  $b$  are smooth functions. Then the finite element solution  $u_h$  satisfies

$$(20) \quad \int_{\Omega_h} \nabla u_h \nabla v dx = \int_{\Omega_h} f v dx \quad \forall v \in S_h^0(\Omega).$$

When  $T_h$  is a uniform three-directional triangulation (generated by the same unit vectors  $t_1, t_2$  and  $t_3$ ), let  $A = \alpha h^2$  and  $h_i = \lambda_i h$  ( $i=1,2,3$ ), the following simplifications occur ([12]) :

- (1) The area integrals (Identity 2.12 in [12]) combine to  $\sum_h^{(n)}(z; u) = \sum_{k=1}^{n-1} h^{2k} \cdot e_h^{(k)}(z; u)$ , where

$$e_h^{(k)}(z; u) = \frac{\lambda_1 \lambda_2 \lambda_3}{4\alpha^2} \beta_k \int_{\Omega} g_h^z(D_1 D_2 D_3 \sum_{i=1}^3 \lambda_i^{2k+1} D_i^3) u dx,$$

$\beta_k \in C_0^1(S_i) \cap C^2(S_i)$  ( $k=2,3$ ),  $D_i$  is the directional derivative along  $S_i$ .

- (2) The remainder terms add up to

$$R_h^{(n)}(z; u) = h^{2n} \sum_{i=1}^3 \frac{\lambda_i^{2n+1} \lambda_{i+2}}{2\alpha} \Phi_i(z; u),$$

where

$$\Phi_i(z; u) = \sum_{K \in T_h} \int_{S_i} \beta_n(s) D_{i+2} g_{3h}^z D_i^6 u ds,$$

and the indices are used mod(3).

Their improved result is the following theorem (Theorem 1 of [12]). We will use this theorem to prove superconvergence.

**Theorem 6.** *If  $u \in C^{2n+\epsilon}(\bar{\Omega})$ , for some  $\epsilon \geq 0$ . Then*

$$(21) \quad u_h(z) = u_I(z) + \sum_{k=1}^{n-1} h^{2k} e_h^{(k)}(z; u) + R_h^n(z; u),$$

where the remainder term is uniformly of the order  $O(h^{2n} |\ln h|)$  if  $\epsilon = 0$ , and  $O(h^{2n})$  if  $\epsilon > 0$ .

As a further by-product of Theorem 6, they gave the following superconvergence result (Corollary 3 of [12]).

**Corollary 6.1.** *If  $u \in C^{4+\epsilon}(\bar{\Omega})$  for some  $\epsilon > 0$ , and if the uniform triangulation consists of equilateral triangles, then there holds*

$$(u - u_h)(z) = O(h^4)$$

*uniformly in nodal points  $z \in \Omega$ .*

On the equilateral triangulation,

$$\lambda_1 = \lambda_2 = \lambda_3 \quad D_1 + D_2 + D_3 = 0,$$

and consequently,  $e_h^{(1)} = 0$ . Then the Corollary 6.1 follows from Theorem 6.

**3.4. Expansion analysis for the superconvergence theory.** As summarized in [15], there are three kinds of approaches to investigating superconvergence properties of finite element methos. One is the Chinese approach based on element analysis ([16] and [17]), with which one can get exact information on the error and derive asymptotic expansions. Moreover, one can prove the global results. It depends on some uniform (with perturbation) properties of the meshes. The second approach is based on the local symmetry of the mesh. It can deal with more general meshes but it can only be able to get interior superconvergence ([4]). The third one is based on numerical valiadtion([18]).We use the idea of Corollary 6.1 but expand the error expression (21) to  $n = 3$  (We need higher smoothness requirement  $C^{6+\epsilon}$ ) rather than  $n = 2$  in Corollary 6.1. Then  $e_h^1 = 0$  and  $e_h^2$  becomes the main error term. We analyze  $e_h^2$  and obtain the following superconvergence result.

**Theorem 7.** *Consider an interior Hexagon pattern 13 vertices-patch (Figure 1)  $\omega_z \subset \subset \Omega_d \subset \Omega$  in the equilateral triangle mesh with  $d = \text{dist}(\omega_z, \partial\Omega_d) \geq Kh$  for some constant  $K$ . Let  $u \in C^{6+\epsilon}(\Omega)$  for some  $\epsilon > 0$  and  $u_h \in S_h$  be the exact and the linear element solution of (19) and (20) respectively. The recovery operator  $G_h$  is defined by PPR on  $\omega_z$ . Then there is a constant  $C$  independent of  $h$  and  $u$  such that*

$$|(\nabla u - G_h u_h)(z)| \leq Ch^4 |\ln h|^{\frac{1}{2}}.$$

*Proof.* By the decomposition in (6), we only need to consider the second term  $|G_h(u_h - u_I)|$ .

The length of equilateral triangle (in vertices 8-9-11 and 7-10-12) side  $S_i$  is  $3h$  and its area  $A = \frac{\sqrt{3}}{4}(3h)^2$ . By the Theorem 6 with  $\lambda_i = 3$  and  $\alpha = \frac{9\sqrt{3}}{4}$ , we have

$$(u_h - u_I)(z) = h^4 e_h^{(2)}(z; u) + R_h^{(3)}(z; u),$$

where

$$e_h^{(2)}(z; u) = 81\beta_2 \int_{\Omega} g_h^z(D_1 D_2 D_3 \sum_{i=1}^3 D_i^3) u dx,$$

$$R_h^{(3)}(z; u) = 486\sqrt{3}h^6 \sum_{i=1}^3 \Phi_i(z; u),$$

$$\Phi_i(z; u) = \sum_{K \in T_h} \int_{S_i} \beta_3(s) D_{i+2} g_h^z D_i^6 u ds.$$

Then

$$(22) \quad G_h(u_h - u_I)(z) = h^4 G_h e_h^{(2)}(z; u) + G_h R_h^{(3)}(z; u).$$

By (3),

$$G_h e_h^{(2)}(z; u) = 81\beta_2 \int_{\Omega} (G_h g_h^z)(D_1 D_2 D_3 \sum_{i=1}^3 D_i^3) u.$$

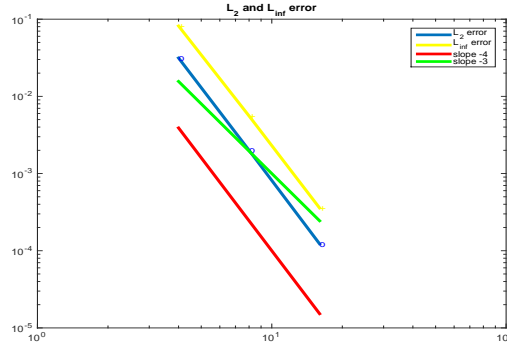


FIGURE 2. Linear element PPR on the Hexagon pattern reaches 4th order convergence for  $L_2$  error and  $L_\infty$  error of  $\nabla u - G_h u$ .

Now  $g_h^z \in S_h$ , and by (7)

$$|G_h g_h^z| \lesssim |g_h^z|_{W^{1,\infty}(\omega_z)}.$$

By Lemma 5,

$$|g_{3h}^z|_{W^{1,\infty}(\omega_z)} \lesssim d^{-1} |\ln h|^{\frac{1}{2}}.$$

Therefore,  $|G_h e_h^{(2)}(z; u)|$  is of order  $h^4 |\ln h|^{\frac{1}{2}}$ , and  $|G_h R_h^{(3)}(z; u)|$  is of higher order at least  $h^5$ . The conclusion follows by applying (6) and (22).  $\square$

**Remark.** As a particular consequence of Lemma 3 in [12] we see that on an equilateral triangulation the Ritz projection of a 5th degree polynomial coincides with its interpolant and  $G_h u_h = \nabla u$  for polynomials with degree less than or equals 4.

**3.5. Numerical example.** Let  $\Omega$  be a hexagon with the center at origin where each side length is 1. The refinement is made by bisecting each side. The initial mesh size is  $h = \frac{1}{2}$ . The equation  $-\Delta u = 2\pi^2 \sin(\pi x) \sin(\pi y)$  satisfies the Dirichlet condition where  $u$  equals the exact solution value  $u(x, y) = \sin(\pi x) \sin(\pi y)$  on the boundary, and  $\omega_z$  is Hexagon pattern 13 vertices-patch (Figure 1). Define the error

$$(23) \quad \begin{aligned} \|\nabla u - G_h u_h\|_{l_\infty(\Omega)} &= \max_{\omega_z \in \Omega} |(\nabla u - G_h u_h)(z)|, \\ \|\nabla u - G_h u_h\|_{l^2(\Omega)} &= \left( \sum_{\omega_z \in \Omega} |(\nabla u - G_h u_h)(z)|^2 \right)^{\frac{1}{2}}. \end{aligned}$$

Superconvergence of 4th order is observed when the hexagon pattern is used (See Table 1 and Figure 2).

TABLE 1. Numerical results of the linear element case on the Hexagon pattern.

Dof	h	$\ \nabla u - G_h u_h\ _{l_\infty(\Omega)}$	order	$\ \nabla u - G_h u_h\ _{l^2(\Omega)}$	order
38	1/4	0.0817	-	0.0315	-
254	1/8	0.0056	3.8749	0.0020	3.972
1262	1/16	0.0004	3.9630	0.0001	4.0275

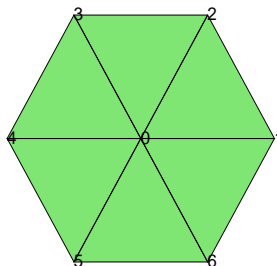


FIGURE 3. Nodes  $n_j$  ( $j=0, \dots, 6$ ) forms a hexagon.

**3.6. Natural superconvergence points on the antisymmetric axis for the linear element in an equilateral triangle mesh.** In one dimension, we have the superconvergence result for the Poisson equation  $-u'' = f$  in the Dirichlet condition that the finite element solution equals the exact solution at nodes. In two dimensions, we find the following exactly equal superconvergence results.

**Theorem 8.** *Let  $\Omega$  be a symmetric domain in  $\mathbb{R}^2$  with respect to a straight line  $l$  that can be discretized by an equilateral triangle mesh. Considering the finite element solution to the Poisson equation  $-\Delta u = f$  with the Dirichlet boundary condition where  $f$  is antisymmetric with respect to  $l$ . That is, if there are 2 points,  $z_1$  and  $z_2$  are symmetric with respect to  $l$ , then  $f(z_1) = -f(z_2)$ . And  $u$  is a constant on this line  $l$ . Then the finite element solution values at the nodes on the antisymmetric axes  $l$  equal their exact solution value on  $l$ .*

*Proof.* Suppose  $u \equiv C_l$  on  $l$ , and without loss of generality, assume  $C_l = 0$  since we can let  $\bar{u} = u - C_l$ . Let the matrix form of the finite element solution be

$$\sum_{j=0}^N a_{ij} u_h(x_j) = b_i \quad (i = 0, \dots, N).$$

Let node  $n_0 \in \text{int}(\Omega)$ ,  $n_j$  ( $j=1, \dots, 6$ ) are nodes adjacent to the node  $n_0$  (Figure 3). Then we compute the load term  $b_{n_0}$  by the quadrature rule.

When  $n_0 \in l$ , nodes  $n_i$  and  $n_k$  ( $1 \leq i, k \leq 6$ ) are symmetric with respect to  $l$ , the antisymmetry of  $f$  with respect to  $l$  gives  $b_{n_0} = 0$  and  $b_{n_i} = -b_{n_k}$ .

A direct calculation by Cramer's Rule and Laplace expansion of  $n_0$ th column leads to

$$u_h(x_{n_0}) = \sum_{n_0 \in l} b_{n_0} A_{n_0} + \sum_{i, k \neq 0} (b_{n_i} + b_{n_k}) A_{ik} = 0,$$

where  $A_{ik}$  are corresponding cofactors. In a general case  $u_h(x_{n_0}) = u(x_{n_0}) \equiv C_l$ .

For example,  $\Omega$  is a hexagon centered at the origin, and the x-axis is the antisymmetric axis for  $f(x, y) = 2\pi^2 \cos \pi x \sin \pi y$ . The linear element solution values at the nodes on the x-axis will then equal their exact solution values.  $\square$

**Remark.** For  $n_0$ th row of the linear element stiff matrix, we have

$$\sum_{j=0}^6 a_{n_0 n_j} u_h(x_{n_j}) = b_{n_0} \quad \text{with} \quad a_{n_0 n_0} = 6a_{n_0 n_j} \quad (j = 1, 2, \dots, 6).$$

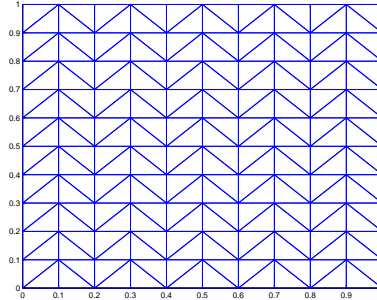


FIGURE 4. Chevron Pattern.

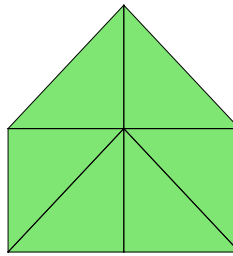


FIGURE 5. Element patch for the Chevron pattern mesh.

**Corollary 8.1.** *Let  $\Omega$  be a symmetric domain in  $\mathbb{R}^2$  with respect to a straight line  $l$  that can be discretized by equilateral triangle mesh. The Poisson equation  $-\Delta u = f + p_2$  satisfies the Dirichlet boundary condition where  $f$  is antisymmetric,  $p_2$  is a polynomial of degree less than or equal to 2, and  $u$  is a constant on this line  $l$ . Then the finite element solution values at the nodes on the antisymmetric axis  $l$  are equal to their exact solution values on  $l$ .*

The Corollary 8.1 follows from Corollary 6.1 and Theorem 8.

#### 4. Quadratic element PPR on the Chevron pattern

Zhang and Naga especially demonstrated the superiority of the PPR over the ZZ patch recovery in [6] by comparing the two under 1) the linear element on the uniform grid of the Chevron pattern ; and 2) the quadratic element on the uniform grid of the regular pattern. Guo and Yang tested the linear element PPR for the wave equation on the Chevron pattern uniform mesh in [8]. This section supplements the quadratic element on the uniform grid of the Chevron pattern, which further verifies the superconvergence stated in Proposition 2. Performing the discrete least squares fitting, we obtain the coefficients of the cubic polynomial at 7 vertices ( $P_j, j=0\dots6$ ) and 12 edge middle points ( $P_j, j=7,\dots,18$ ) of the scaled patch  $\omega_z$  in Figure 5 with vertex 0 being the patch center  $z$ . Therefore the recovered gradient on the patch  $G_h u_h(x, y) = \nabla p_3(x, y)$ . By Taylor expansion analysis in the

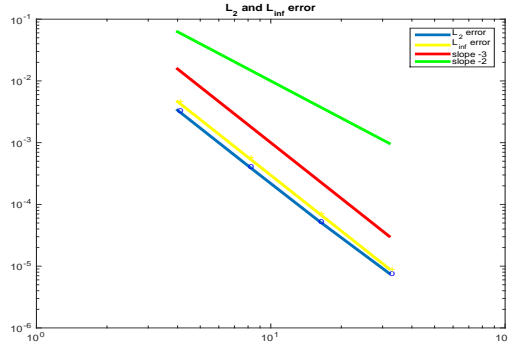


FIGURE 6. Quadratic element PPR convergence rate on the Chevron pattern for Possion equation:  $L_2$  and  $L_{inf}$  errors of  $\nabla u - G_h u$ .

local reference coordinate,

(24)

$$|(G_{hx}u_I - \frac{\partial u}{\partial x})(0,0)| = \frac{h^3}{912} \frac{\partial^4 u}{\partial^3 x \partial y} + \frac{11h^3}{450} \frac{\partial^4 u}{\partial x \partial^3 y} + O(h^4),$$

$$|(G_{hy}u_I - \frac{\partial u}{\partial y})(0,0)| = \frac{191h^3}{210192} \frac{\partial^4 u}{\partial^3 x \partial y} + \frac{31043h^3}{420384} \frac{\partial^4 u}{\partial x \partial^3 y} + \frac{1081h^3}{420384} \frac{\partial^4 u}{\partial^4 y} + O(h^4).$$

**4.1. Numerical results for the Possion equation.** In this section, we numerically illustrate our result for the quadratic element on the Chevron pattern. In the first numerical example, we consider the Possion equation with a polynomial on the right hand side.

(25)

$$-\Delta u = 2(x + y - x^2 - y^2) \quad \text{in } \Omega,$$

$$u = 0 \quad \text{on } \partial\Omega.$$

where  $\Omega = [0, 1]^2$ .  $l_2(\Omega)$  error is defined the same as (23), and we fixed the inner point  $z = (0.5, 0.5)$  for testing local absolute value error  $l_{inf}(z) = |(\nabla u - G_h u_h)(z)|$ .

Table 2 and Figure 6 shows the superconvergence of 3rd order.

TABLE 2. Quadratic element on Chevron pattern for Possion equation.

Dof	h	$ (\nabla u - G_h u_h)(z) $	order	$\ \nabla u - G_h u_h\ _{L^2(\Omega)}$	order
18	1/4	$4.6 \times 10^{-3}$	-	$3.4 \times 10^{-3}$	-
98	1/8	$6.0 \times 10^{-4}$	2.9972	$4.0 \times 10^{-4}$	2.9936
450	1/16	$7.3 \times 10^{-5}$	2.9987	$5.4 \times 10^{-5}$	2.9561
1922	1/32	$9.1 \times 10^{-6}$	2.9997	$7.7 \times 10^{-6}$	2.8257

**4.2. Numerical results for the wave equation.** Guo and Yang generalized the study of PPR to the wave equation ([8]). They presented a numerical example of the linear element PPR for the wave equation on the Chevron pattern. We now consider the following linear wave equation (5.1 of [8]) and add a numerical example

of quadratic element PPR.

$$\begin{aligned}
 & \frac{\partial^2 u}{\partial t^2} - \Delta u = f \quad \text{in } (x, t) \in \Omega \times (0, 1], \\
 & u = 0 \quad \text{on } (x, t) \in \partial\Omega \times (0, 1], \\
 (26) \quad & u(x, 0) = \sin(\pi x) \sin(\pi y) \quad x \in \Omega, \\
 & \frac{\partial u}{\partial t}(x, 0) = -\sin(\pi x) \sin(\pi y) \quad x \in \Omega,
 \end{aligned}$$

where  $\Omega = [0, 1]^2$ , and  $f$  is chosen to fit the exact solution  $u(x, t) = e^{-t} \sin(\pi x) \sin(\pi y)$ . By [19], the error is bounded by  $C(h^k + \delta t^2)$  in each discrete time case, where  $\delta t$  is the time step. We take the time step as the square of the space size, i.e.,  $\delta t = h^2$ . To get superconvergence of the quadratic element, one needs higher order time discretization, and thus we choose the fourth order time discretization used in [8] which can be reformulated into a predictor-correct form. The predictor step is

$$(v_h, w_h) + (\nabla u_h^n, \nabla w_h) = (f^n, w_h) \quad w_h \in S_h^0(\Omega),$$

and the correct step is

$$\begin{aligned}
 (27) \quad v_h &= \frac{u_h^* - 2u_h^n + u_h^{n-1}}{\delta t^2}, \\
 (u_h^{n+1}, w_h) &= (u_h^*, w_h) - \frac{\delta t^4}{12} (\nabla v_h, \nabla w_h) \quad w_h \in S_h^0(\Omega).
 \end{aligned}$$

Note the above scheme needs initial conditions of two time steps. As in [8], we consider the Taylor expansion of  $u$  at  $t = 0$ ,

$$u(., \delta t) = u(., 0) + \delta t \frac{\partial u}{\partial t}(., 0) + \frac{\delta t^2}{2} \frac{\partial^2 u}{\partial t^2}(., 0) + O(\delta t^3).$$

We compute the numerical error at time  $T = 1$ .  $l_2(\Omega)$  error is defined the same as (23), and we again fix the inner point  $z = (0.5, 0.5)$  for test local absolute value error  $l_{inf}(z) = |(\nabla u - G_h u_h)(z)|$ . Table 3 lists errors and convergence rates of the numerical solution for the quadratic element on the Chevron pattern uniform mesh.

TABLE 3. Quadratic element on the Chevron pattern for wave equation.

Dof	h	$ (\nabla u - G_h u_h)(z) $	order	$\ \nabla u - G_h u_h\ _{l^2(\Omega)}$	order
18	1/4	0.033	-	0.017	-
98	1/8	0.0056	2.5556	0.0026	2.6727
450	1/16	0.0007	3.0541	0.0003	3.1463

### 5. Conclusions

In this work, we further investigate the Polynomial Preserving Recovery (PPR) post-processing technique for finite element methods. Our main results are listed as following:

- (1) A hexagon patch is designed for the equilateral triangular mesh on which PPR is applied on the linear element to achieve  $h^4 |\ln h|^{\frac{1}{2}}$  superconvergence for the recovered gradient. An exact equal superconvergence phenomenon is also investigated on this mesh.
- (2) An interior maximum norm estimates for the discrete Green's function is given to relax the global regularity assumption on the solution.

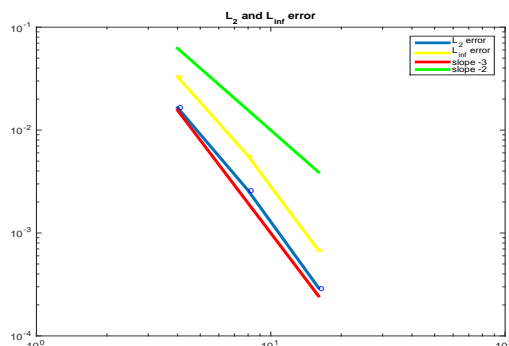


FIGURE 7. Quadratic element PPR convergence rates on the Chevron pattern for the wave equation:  $L_2$  and  $L_{inf}$  errors of  $\nabla u - G_h u$ .

- (3) A quadratic element PPR on the Chevron pattern mesh with an application to a wave equation is implemented to verify the previous superconvergence theory.

### Acknowledgments

This work was conducted at Wayne State University, USA. The first author was supported by the Young Scholar Training Program of Shandong Province. The authors thank Prof. Wenming He of Lingnan Normal University for helpful discussion about discrete Green function. The authors also thank Dr. Hailong Guo of the University of Melbourne for sharing his solving wave equation MATLAB code package.

### References

- [1] Wang, F. and Han, W., Reliable and Efficient a Posteriori Error Estimates of DG Methods for a Simplified Frictional Contact Problem, *International Journal of Numerical Analysis and Modeling*, vol.16(1), pp.49-62, 2019.
- [2] Yang, W., Cao, L., Huang, Y. and Cui, J., A New Posteriori Error Estimate for the Interior Penalty Discontinuous Galerkin Method, *International Journal of Numerical Analysis and Modeling*, vol.16(2), pp.210-224, 2019.
- [3] Zhu, Q. and Lin, Q., *Finite Element Superconvergence Theory* (in Chinese), Hunan Science and Technology Press, 1989.
- [4] Wahlbin, L.B., *Superconvergence in Galerkin Finite Element Methods*, Vol.1605, Springer, Berlin, 1995.
- [5] Zienkiewicz, O.C and Zhu, J., The Superconvergent Patch Recovery and a Posteriori Error Estimates. Part 1: The Recovery Technique, *International Journal for Numerical Methods in Engineering*, vol.33, pp.1331-1364, 1992.
- [6] Zhang, Z and Naga, A., A New Finite Element Gradient Recovery Method: Superconvergence Property, *SIAM J. Sci. Comput.*, Vol.26(4), pp.1192-1213, 2005.
- [7] Zhang, Z, Recovery Techniques in Finite Element Methods, in: *Adaptive Computations: Theory and Algorithms*, eds. Tang, T and Xu, J, Mathematics Monograph Series 6, Science Publisher, pp.333-412, 2007.
- [8] Guo, H. and Yang, X., Polynomial Preserving Recovery for High Frequency Wave Propagation, *J. Sci. Comput.*, Vol.71(2), pp.594-614, 2017.
- [9] Wang, L., Zhang, Q. and Zhang, Z., Superconvergence Analysis and PPR Recovery of Arbitrary Order Edge Elements for Maxwell's Equations, *J. Sci. Comput.*, Vol.78(2), pp.1207-1230, 2019.

- [10] Du, Y. and Zhang, Z., Supercloseness of Linear DG-FEM and Its Superconvergence Based on the Polynomial Preserving Recovery for Helmholtz Equation, *J. Sci. Comput.*, Vol.79(3), pp.1713-1736, 2019.
- [11] Guo, H., Xie, C. and Zhao, R., Superconvergent gradient recovery for virtual element methods, *Mathematical Models and Methods in Applied Sciences*, 2019. <https://doi.org/10.1142/S0218202519500386>.
- [12] Blum, H., Lin, Q. and Rannacher, R., asymptotic Error Expansion and Richardson Extrapolation for Linear Finite Elements, *Numer. Math.*, Vol.49, pp.11-37, 1986.
- [13] Naga, A. and Zhang, Z., A Posteriori Error Estimates Based on the Polynomial Preserving Recovery, *SIAM Journal on Numerical Analysis*, Vol.42(4), pp.1780-1800, 2004.
- [14] Schatz, A.H. and Wahlbin, L.B., Interior Maximum-Norm Estimates for Finite Element Methods, Part II, *Mathematics of Computation*, Vol.64(211), 1995.
- [15] Huang, Y., Shu, S. and Yu, H., Superconvergence and Asymptotic Expansions for Linear Finite Element Approximations on Crisscross Mesh, *Science in China Series A: Mathematics*, Vol.47(1), pp.136-145, 2004.
- [16] Chen, C. and Huang, Y., *High Accuracy Theory of Finite Element Methods* (in Chinese), Hunan Science and Technology Press, Changsha, China, 1995.
- [17] Lin, Q. and Yan, N., *The Construction and Analysis of High Efficient Finite Element Methods* (in Chinese), Hebei University Press, Baoding, China, 1996.
- [18] Babuška, I., Strouboulis, T., Upadhyay, C. S. and Gangaraj, S. K., Computer-based proof of the Existence of Superconvergence Points in the Finite Element Method; Superconvergence of the Derivatives in Finite Element Solutions of Laplace's, Poisson's, and the Elasticity Equations, Vol.12, pp.347-392, 1996.
- [19] Dupont, T.,  $L^2$ -Estimates for Galerkin Methods for Second Order Hyperbolic Equations, *SIAM Journal on Numerical Analysis*, Vol.10(5), pp.880-889, 1973.

Department of Applied Mathematics, Shandong Agricultural University, Taian, 271018, China  
*E-mail:* [pan\\_hao2003@163.com](mailto:pan_hao2003@163.com)

Department of Mathematics, Wayne State University, Detroit, MI 48202, USA  
*E-mail:* [zzhang@math.wayne.edu](mailto:zzhang@math.wayne.edu) and [zhao.lewei@wayne.edu](mailto:zhao.lewei@wayne.edu)  
*URL:* <https://www.math.wayne.edu/zzhang/>  
*URL:* <http://sites.google.com/site/leweizhaomath/>